ORIGINAL PAPER

CrossMark

Modeling and mapping of soil salinity in Tafilalet plain (Morocco)

Mohammed El hafyani[1] · Ali Essahlaoui[1] · Mohamed El baghdadi[2] · Ana C. Teodoro[3] · Meriame Mohajane[1,4] · Abdellah El hmaidi[1] · Abdelhadi El ouali[1]

Abstract
The Tafilalet plain in Morocco is a very rich ecosystem. It presents enormous ecological and natural values, such as groundwater and agricultural soil; however, it is undergoing rapid changes due to natural and anthropogenic factors, where soil salinity constitutes one of the major problems. In this context, remote sensing data/techniques used to map and to model soil salinity is a valuable tool in management activities and in decision-making. This paper focuses on modeling and mapping soil salinity in Tafilalet plain, Morocco, based on Landsat 8 OLI satellite data in combination with ground field data. Our results indicated that the coefficient of determination (R^2) varies from 0.53 to 0.75 and the Root Mean Square Error (RMSE) ranges between 0.62 and 0.80 dS/m. Based on the results, we can conclude that this approach is an effective and valid methodology for modeling and spatial mapping soil salinity in this area and this method could also be applied for other regions with similar characteristics.

Keywords Tafilalet plain · Landsat 8 OLI · Electrical conductivity · Soil salinity

Introduction

Nowadays, soil salinity has become a serious worldwide environmental and socio-economic problem (Sidike et al. 2014), mainly in arid and semi-arid zones (FAO 2002; Farifteh et al. 2006; Rengasamy 2006; Wang et al. 2012; Abbas et al. 2013; Ibrahim 2016; Allbed et al. 2014; EL Harti et al. 2016) because of several factors which include soil factors (parent material, permeability, water table depth, groundwater quality, and topography); management factors (irrigation and

drainage); and climatic factors (rainfall and humidity) (Ug and Ahmed Douaik 2008) cited in Allbed et al. (2014). So, reducing the risk of soil salinity disasters is essential for protecting environment and reducing economic losses in terms of agriculture (Allbed and Kumar 2013).

Conventional studies for modeling and mapping soil salinity are usually based on ground-based measurements and laboratory analyses (Norman et al. 1989) cited in Dehaan and Taylor (2002; however, these methods are costly, time-consuming, and difficult to apply for large areas because they are not accessible for repeatable sampling (Bannari et al. 2008; Lhissou et al. 2014; Barbouchi et al. 2014; Farifteh et al. 2007a, b; EL Harti et al. 2016). To overcome this limitation, several researchers have made great efforts, experienced worldwide, in developing advanced methods and techniques based on remote sensing data/techniques for mapping, monitoring, and understanding soil salinity processes (Bannari et al. 2008; Allbed and Kumar 2013).

Different data such as satellite images, airborne imagery, and in-situ spectroradiometry data have been used in different contexts for soil salinity mapping (e.g., Farifteh et al. 2007a, b; EL Harti et al. 2016; Chaturvedi et al. 1983; Singh and Srivastav 1990; Russell 1990; Taylor et al. 1996; Metternicht 1998; Dehaan and Taylor (2002; Metternicht and Zinck 2003).

Previous studies, such as those conducted by Dehaan and Taylor (2002), Khan et al. (2005), Bouaziz et al. (2011),

✉ Mohammed El hafyani
elhafyani.91med@gmail.com

1 Department of Geology, Laboratory of Geoengineering and environment, Research Group "Water Sciences and Environment Engineering", Faculty of Sciences, Moulay Ismail University, Zitoune, BP11201 Meknès, Morocco

2 Laboratory of Geo-resources and Environment, Department of Geology, Faculty of Science and Technology, My Slimane University, Béni Mellal, Morocco

3 Earth Sciences Institute (ICT) and Department of Geosciences, Environment and Land Planning, Faculty of Sciences, University of Porto, Porto, Portugal

4 Department of Biology, Research Group "Soil and Environnement Microbiology Unit", Faculty of Sciences, Moulay Ismail University, Zitoune, BP11201 Meknès, Morocco

Abbas et al. (2013), Hamzeh et al. (2012), and Allbed et al. (2014) focused on combining different spectral indices derived from several sensors with geochemical laboratory measurements.

In this context, this study aimed to apply remote sensing data combined with ground field measurements to model and to map soil salinity and thereby contribute to increase scientific understanding of the influence of soil salinity on agriculture in the Tafilalet plain region (Morocco).

Materials and methods

Study area

The study area (216 ha) belongs to Tafilalet plain (Morocco), that have a total surface of 20,000 ha. Geologically, the area consists of Quaternary terrains on top of the Paleozoic basement. It is under the Saharan influences towards the south and this is favored by the relative lowering of the Eastern Anti-Atlas, so the eastern winds easily reach the sector. According to Joly (1962), the climate is a "Mediterranean-Saharan." In Erfoud station, the dry period lasts almost all the year with a very hot summer and a very cold winter (Fig. 1), with average temperature varying from 9 to 34 °C. The mean annual evapotranspiration is 1371 mm and remains higher than the annual rainfall (60.3 mm) which indicates that the region experienced a water deficit all over the year. The soil in the study area is generally subdesirtic (Billaux and Bryssine 1966) with a silty texture, and the agricultural practice is usually done by irrigation.

Due to the practical impossibility to perform field work in all the Tafilalet plain area, and in order to take all the samples needed in the same day, we collect 25 samples within the study area, considering a sample area of 216 ha (Fig. 2c)). The samples were taken in the south-western part of the Tafilalet plain, which extends from a few kilometers north of Erfoud to the south of Rissani, close to the main river Ziz that supplies this plain. This area is assumed to be representative of the study area characteristics.

Data

In this study, one Operational Land Imager (OLI) (path200/row38) image, acquired on February 09, 2016, downloaded from the United States Geological Survey (USGS) website, was considered. The OLI sensor recorded information in 11 bands (Table 1); however, in our research, only the visible bands (bands 2–4) and the Near Infrared band (NIR) (band 5) were considered.

Ground truth samples were taken in 25 points distributed over the study area (Fig. 2), where Electrical Conductivity (EC) was measured by chemical process at the laboratory facilities.

Methodology

The methodology adopted aimed to map the soil salinity in the Tafilalet plain by integrating remote sensing data and field measurements. This study was subdivided into five main steps: (1) Landsat OLI image downloaded, preprocessing data, study area extraction; (2) integration of several parameters including the visible bands (bands
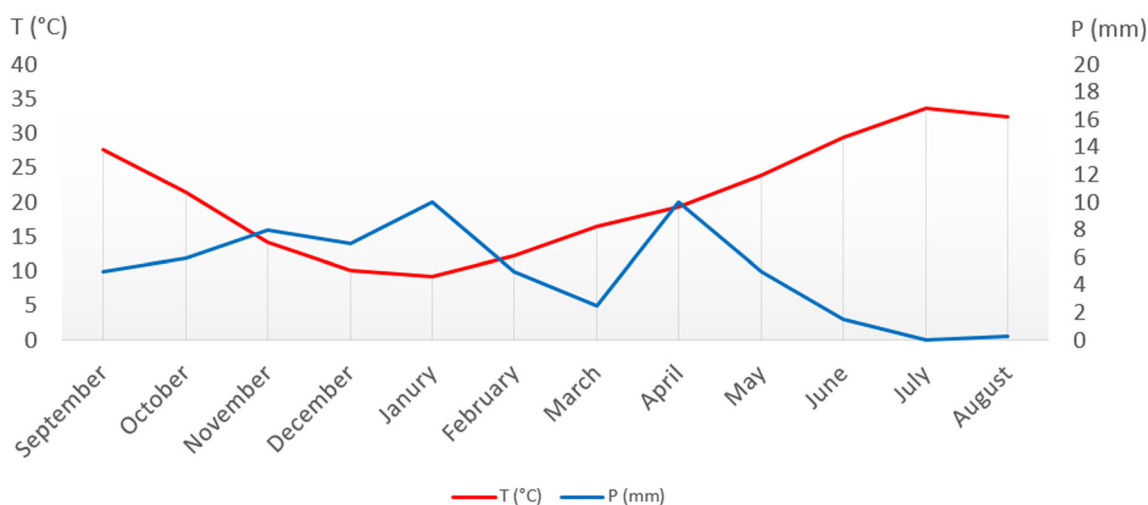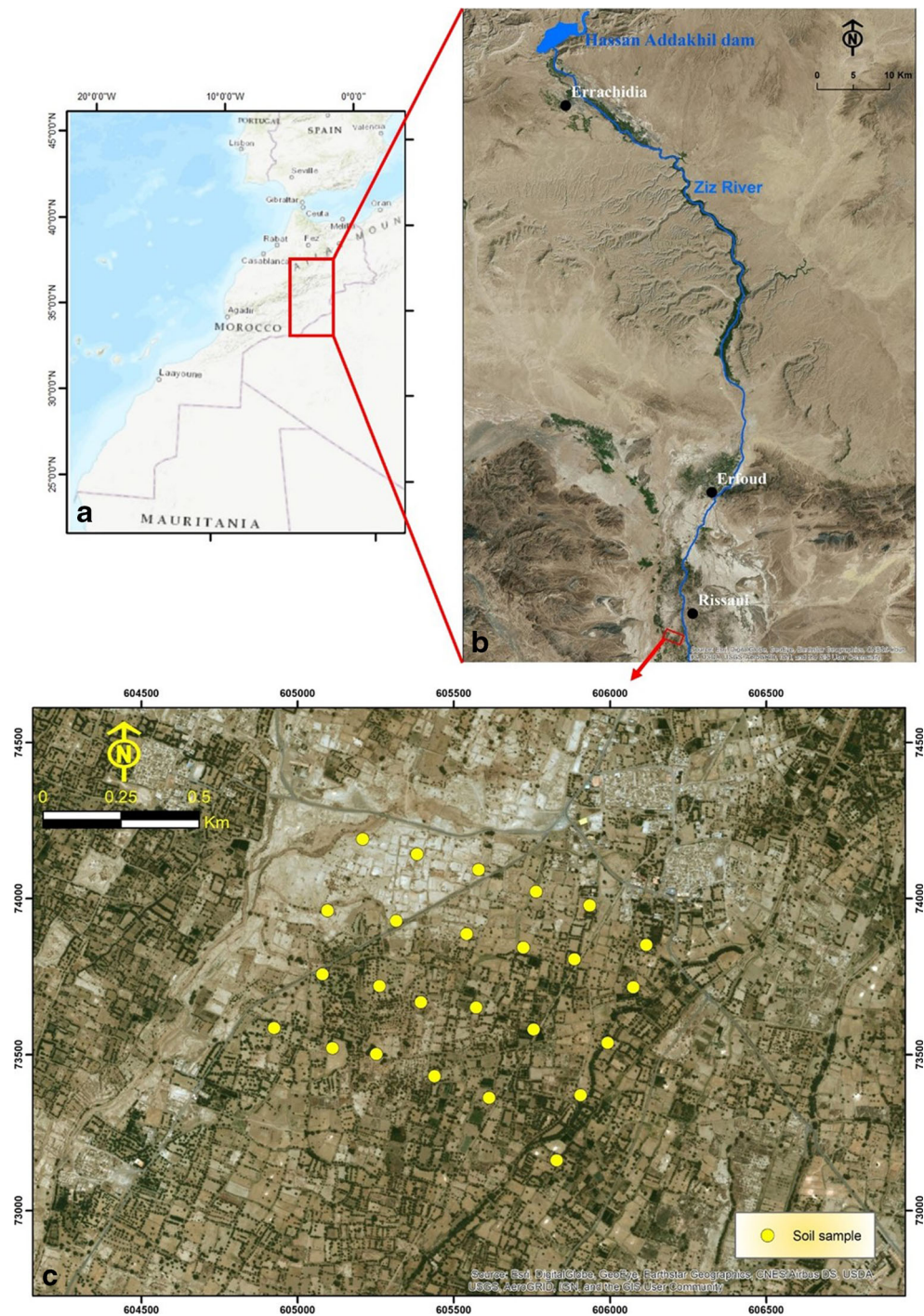

Fig. 1 Ombrothermal diagram in Erfoud station during the hydrological years 1982 to 2002

Fig. 2 **a** and **b** Localization of the study area; **c** soil sample locations taken within the area assigned by a red rectangle in **b**.

2–4), the NIR band (band 5), and the Salinity Index; (3) integration of field measurements; (4) statistical analysis and modeling; and (5) selection of most appropriate model and computation of the spatial mapping of salinity. An outline of the methodology employed is shown in Fig. 3.

Chemical analysis

The measurements of the EC were performed in the laboratory, considering the following procedure: (Sidike et al. 2014) 5 g of soil sample prepared for the test was weighed and placed in a polyethylene plastic bags;

Table 1   Spectral bands of Landsat 8 OLI

Bands	Wavelength (micrometers)	Resolution (meters)
Band 1: Ultra Blue (coastal/aerosol)	0.43–0.45	30
Band 2: Blue	0.45–0.51	30
Band 3: Green	0.53–0.59	30
Band 4: Red	0.64–0.67	30
Band 5: Near Infrared (NIR)	0.85–0.88	30
Band 6: Shortwave Infrared (SWIR) 1	1.57–1.65	30
Band 7: Shortwave Infrared (SWIR) 2	2.11–2.29	30
Band 8: Panchromatic	0.50–0.68	15
Band 9: Cirrus	1.36–1.38	30

Table 2   Conventional intervals of the soil EC (Yu et al. 2010)

Categories	EC minimum (dS/m)	EC maximum (dS/m)
Non-saline soil	0	2
Slightly saline soil	2	4
Moderately saline soil	4	8
Strongly saline soil	8	16

(FAO 2002) 40 ml of distilled water was added; and (Farifteh et al. 2006) the flask was closed and placed in the mechanical stirrer with horizontal movement for 30 min. After filtration, the conductivity of the solution obtained was measured by conductivity meter.

Salinity index

The Salinity Index (SI), is a spectral index proposed by Khan et al. (2005) and presented in Eq. (1).

$$SI = \sqrt{B \times R} \qquad (1)$$

Where, B is referred to blue band and R to red band.

This index was already applied for other authors with good results (Bouaziz et al. 2011; Abbas et al. 2013; Allbed and Kumar 2013; Lhissou et al. 2014; El Harti et al. 2016).

Regression analyseis and validation

A linear regression was established in order to examine the relationship between the EC measured in the field and several variables derived by remote sensing (the Blue, Green, Red and NIR bands and the salinity index). The validation of the models was performed considering the coefficient of determination (R^2), the root mean square error (RMSE) and p values.

According to conventional intervals of the soil EC adopted in the literature (Shirokova et al. 2000; Farifteh et al. 2008; Yu et al. 2010; EL Harti et al. 2016), four categories were considered, as presented in Table 2.

Results and discussion

Model validation and evaluation

The EC estimation models (Fig. 5) and their statistical parameters, presented in Fig. 4 and Table 3, respectively, allowed to map and model EC through the computation of linear regressions. Multiple stepwise regression analysis allowed to generate different models that are suitable for mapping soil salinity, as well as the parameters incorporated in each one (Table 3). The different models showed a heavy exploit of the spatial mapping of the soil salinity and a strong correlation between the EC estimated and the various parameters integrated (visible and NIR bands) and the salinity index. The green band was discarded due to its lower correlation with the EC ($R^2 = 0.49$) and also due its weak correlation with the salinity index. The

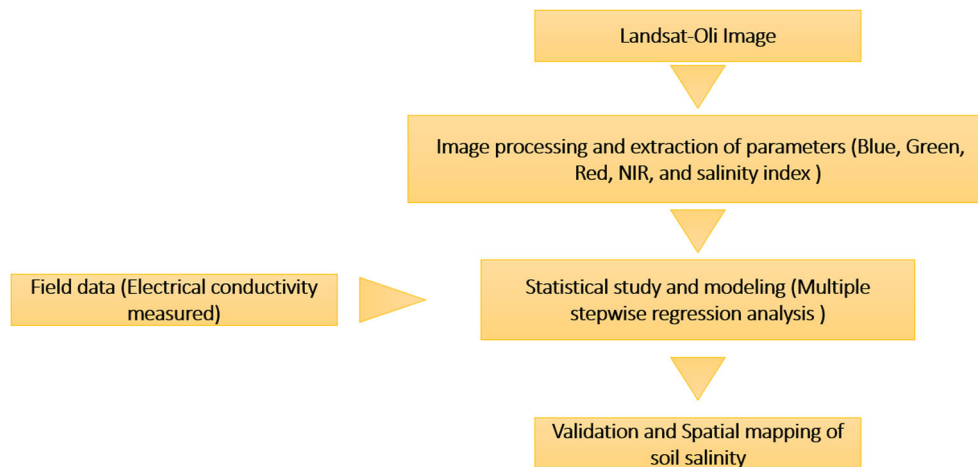**Fig. 3** Flowchart of the methodology employed

Landsat-Oli Image

Image processing and extraction of parameters (Blue, Green, Red, NIR, and salinity index)

Field data (Electrical conductivity measured)

Statistical study and modeling (Multiple stepwise regression analysis)

Validation and Spatial mapping of soil salinity

Fig. 4 EC measured versus EC estimated through the models (best models performance)
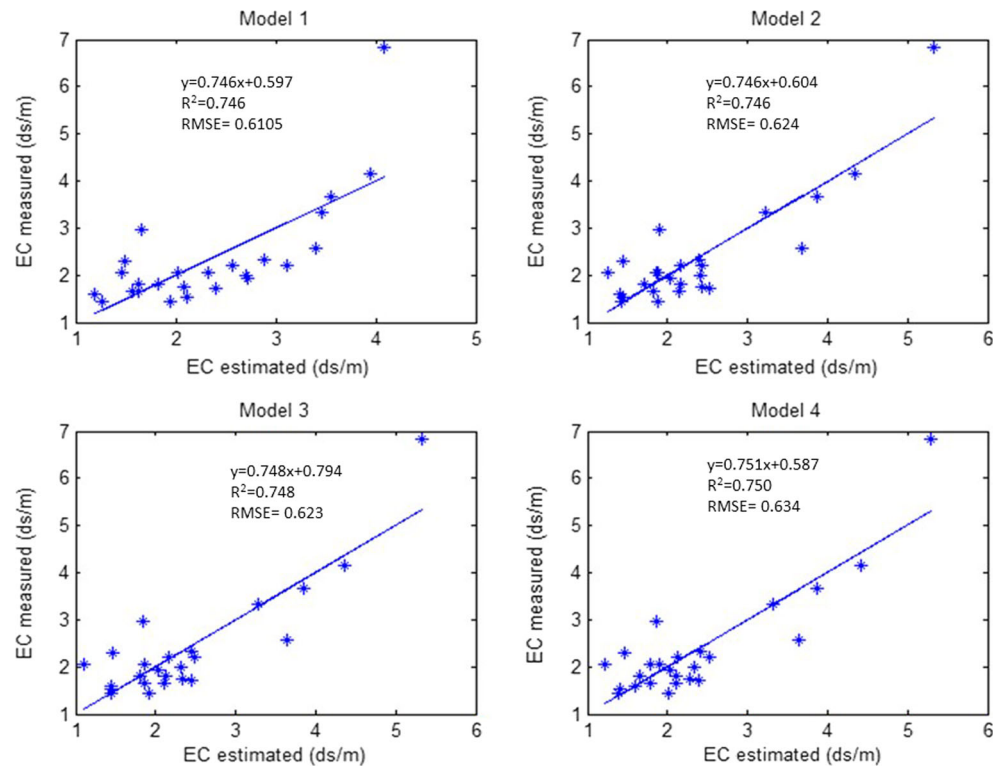
Table 3 Statistical parameters of the best performance models

Model	Variables	R^2	RMSE (dS/m)	p value	Model equation
1	SI, NIR	0.746	0.6105	2.77×10^{-6}	$EC = -114{,}919*SI + 260{,}710*NIR - 19{,}7785$
2	SI, NIR, BLUE	0.746	0.624	1.81×10^{-6}	$EC = -117{,}35*SI + 245{,}92*NIR + 14{,}91*BLUE - 19{,}25$
3	SI, NIR, RED	0.748	0.623	1.71×10^{-6}	$EC = -183{,}104*SI + 294{,}417*NIR - 36{,}2106*RED - 20{,}538$
4	SI, NIR, BLUE, RED	0.750	0.634	7.73×10^{-6}	$EC = -298{,}205*SI + 236{,}621*NIR + 106{,}927*BLUE + 88{,}061*RED - 17{,}885$

correlation matrix shows a strong correlation between the salinity index and the other two visible bands (blue and red) (Table 4).

3.1 Spatial variation salinity

The EC map (Fig. 5) was generated based on the Model 4 equation ($EC = -298{,}205*SI + 236{,}621*NIR + 106{,}927*BLUE + 88{,}061*RED - 17{,}885$), considering the integration of different variables. The results show that 1.37 ha

Table 4 Correlation matrix

	SI	Blue	Red
SI	1.000	0.997	0.998
Blue	0.997	1.000	0.997
Red	0.998	0.997	1.000

of soil is not affected by salinity, 156.89 ha is slightly saline plots, 60.88 ha is moderately saline soil, and 0.74 ha is strongly saline soil. In order to classify the built-up area (Fig. 5), a supervised classification method was employed; however, certain built-up areas were misclassified. The reason could be related to the similar spectral signatures of land cover in this area. Hence, the built-up areas were digitized from Google Earth images.

The study area suffered a greater salinity of soils especially in its northeast part (Fig. 5). Moreover, it is at this level that the ranges of the EC qualify this area as "saline soils" (EC > 8 ds/m), as can be seen in Table 2. The southern part of the study area is dominated by two classes; non-saline soils and slightly saline soils (EC ranges between 0 and 4 ds/m), with the presence of some beaches of the class of moderately saline soils.

The comparison of the results of the model and the field data shows the same trend and the same distribution of salinity

Fig. 5 EC-based model considered (Model 4)
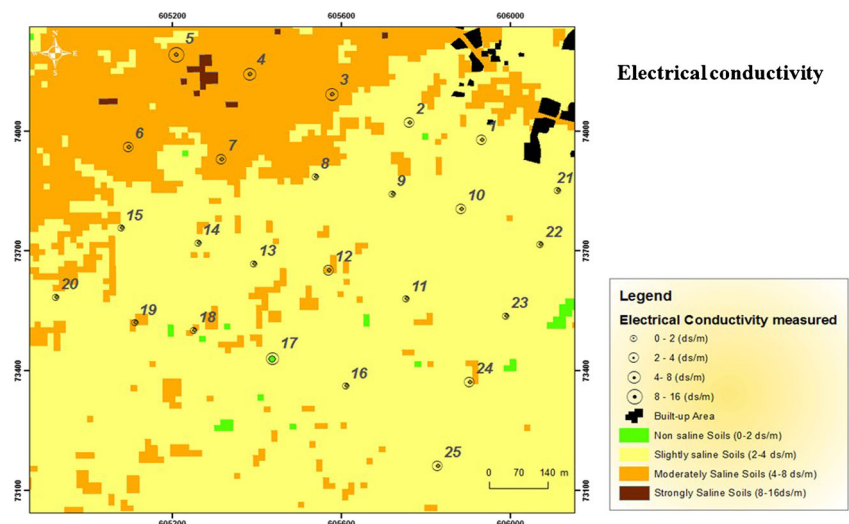
levels. Indeed, both show the existence of an increasing degree of salinity from South to North.

There is, therefore, a good agreement in the different degrees of soil salinity between the EC estimated and the EC measured. The best model shows a very high compliance index ($R^2 = 0.75$), a RMSE of 0.68, and it is generated by the intervention of majority of parameters (the bands Blue, Red and NIR, and the salinity index), indicating a good perception of the remote sensing data in the spatial mapping of soil salinity.

Several works have been carried out under this scope, which have demonstrated the usefulness of satellite imagery in mapping, modeling, and spatio-temporal monitoring of soil salinity. For instance, Allbed and Kumar (2013) applied a modeling and a spatial mapping of soil salinity in Oasis El Hassa in Saudi Arabia. They showed that the combination of the Red band of the IKONOS sensor and the salinity index is a very efficient method for the spatial mapping of salinity and explain 65% of the spatial variation in soil salinity of the study area.

El Harti et al. (2016) used Landsat TM and OLI data combined with in-situ EC measurements in order to propose a spatio-temporal monitoring method of soil salinity in the Tadla plain, in central Morocco. They were able to demonstrate that the integration of visible bands of Landsat sensors has strengthened the OLI-SI index and allowed a good characterization of saline soils.

Conclusion

This study aims to model and map the soil salinity in an area within the Tafilalet plain by integrating remote sensing data and field measurements. Our results indicated that the R^2 varies from 0.53 to 0.75 and the RMSE ranges between 0.62 and 0.80 dS/m. Based on the results, we can conclude that the ability of Landsat-8 OLI data associated with in situ CE measurements to map soil salinity has been proven to be suitable.

This research provides information for management decisions and thereby supports the development and implementation of sustainable agriculture policies.

Compliance with ethical standards

Conflict of interest   The authors declare that they have no conflict of interest.

References

Abbas A et al (2013) Characterizing soil salinity in irrigated agriculture using a remote sensing approach. Phys Chem Earth 55–57:43–52, Elsevier Ltd. https://doi.org/10.1016/j.pce.2010.12.004

Allbed A, Kumar L (2013) Soil salinity mapping and monitoring in arid and semi-arid regions using remote sensing technology: a review. Adv Remote Sens 2(December):373–385. https://doi.org/10.4236/ars.2013.24040

Allbed A, Kumar L, Sinha P (2014) Mapping and modelling spatial variation in soil salinity in the Al Hassa Oasis based on remote sensing indicators and regression techniques. Remote Sens 6(2): 1137–1157. https://doi.org/10.3390/rs6021137

Bannari A, Guedon AM, el-Harti A, Cherkaoui FZ, el-Ghmari A (2008) Characterization of slightly and moderately saline and sodic soils in irrigated agricultural land using simulated data of advanced land imaging (EO-1) sensor. Commun Soil Sci Plant Anal 39(19–20): 2795–2811. https://doi.org/10.1080/00103620802432717

Barbouchi, M., Abdelfattah, R., Chokmani, K., Aissa, N. B., Lhissou, R., & El Harti, A. (2015) Soil salinity characterization using polarimetric InSAR coherence: Case studies in Tunisia and Morocco. IEEE Journal of Selected Topics in Applied Earth Observations and Remote Sensing, 8(8), 3823–3832

Billaux P, Bryssine G (1966) Les sols du Maroc

Bouaziz M, Matschullat J, Gloaguen R (2011) Improved remote sensing detection of soil salinity from a semi-arid climate in Northeast

Brazil. Compt Rendus Geosci 343(11–12):795–803. https://doi.org/10.1016/j.crte.2011.09.003

Chaturvedi L et al (1983) Multispectral remote sensing seeps. IEEE Trans Geosci Remote Sens 21(3):239–251

Dehaan RL, Taylor GR (2002) Field-derived spectra of salinized soils and vegetation as indicators of irrigation-induced soil salinization. Remote Sens Environ 80(3):406–417. https://doi.org/10.1016/S0034-4257(01)00321-2

El Harti A et al (2016) Spatiotemporal monitoring of soil salinization in irrigated Tadla Plain (Morocco) using satellite spectral indices. Int J Appl Earth Obs Geoinf 50:64–73, Elsevier B.V. https://doi.org/10.1016/j.jag.2016.03.008

FAO (2002) WFS:fyl Focus on the issues

Farifteh J, Farshad A, George RJ (2006) Assessing salt-affected soils using remote sensing, solute modelling, and geophysics. Geoderma 130(3–4):191–206. https://doi.org/10.1016/j.geoderma.2005.02.003

Farifteh J, van der Meer F, Atzberger C, Carranza EJM (2007a) Quantitative analysis of salt-affected soil reflectance spectra: a comparison of two adaptive methods (PLSR and ANN). Remote Sens Environ 110(1):59–78. https://doi.org/10.1016/j.rse.2007.02.005

Farifteh J, van der Meer F, Carranza EJM (2007b) Similarity measures for spectral discrimination of salt-affected soils. Int J Remote Sens 28(23):5273–5293. https://doi.org/10.1080/01431160701227604

Farifteh J, van der Meer F, van der Meijde M, Atzberger C (2008) Spectral characteristics of salt-affected soils: a laboratory experiment. Geoderma 145(3–4):196–206. https://doi.org/10.1016/j.geoderma.2008.03.011

Hamzeh S et al (2012) Estimating salinity stress in sugarcane fields with spaceborne hyperspectral: vegetation indices. Int J Appl Earth Obs Geoinf 21(1):282–290, Elsevier B.V. https://doi.org/10.1016/j.jag.2012.07.002

Ibrahim M (2016) Modeling soil salinity and mapping using spectral remote sensing data in the arid and semi-arid region. Int J Remote Sens Appl 6:76. https://doi.org/10.14355/ijrsa.2016.06.008

Joly F (1962) Etudes sur le relief du Sud-Est Marocain: thèse pour le doctorat ès Lettres présentée à la Faculté des lettres et Sciences humaines de l'Université de Paris

Khan NM, Rastoskuev VV, Sato Y, Shiozawa S (2005) Assessment of hydrosaline land degradation by using a simple approach of remote sensing indicators. Agric Water Manag 77(1–3):96–109. https://doi.org/10.1016/j.agwat.2004.09.038

Lhissou R, El A, Chokmani K (2014) Mapping soil salinity in irrigated land using optical remote sensing data. Eur J Soil Sci 3(2):82–88

Metternicht GI (1998) Fuzzy classification of JERS-1 SAR data: an evaluation of its performance for soil salinity mapping. Ecol Model 111(1):61–74. https://doi.org/10.1016/S0304-3800(98)00095-7

Metternicht GI, Zinck JA (2003) Remote sensing of soil salinity: potentials and constraints. Remote Sens Environ 85(1):1–20. https://doi.org/10.1016/S0034-4257(02)00188-8

Norman CP, Lyle CW, Heuperman AF, & Poulton D (1989) Tragowel plains–challenge of theplains. Tragowel plains salinity management plan, soil salinity survey, Tragowel Plains Subregional workinggroup 49-89.

Rengasamy P (2006) World salinization with emphasis on Australia. J Exp Bot 57(5):1017–1023. https://doi.org/10.1093/jxb/erj108

Russell WGR (1990) Some spectral considerations for remote sensing of soil salinity. Aust J Soil Res 28:417–431

Shirokova Y, Forkutsa I, Sharafutdinova N (2000) Use of electrical conductivity instead of soluble salts for soil salinity monitoring in Central Asia. Irrig Drain Syst 14(3):199–205. https://doi.org/10.1023/A:1026560204665

Sidike A, Zhao S, Wen Y (2014) Estimating soil salinity in Pingluo County of China using QuickBird data and soil reflectance spectra. Int J Appl Earth Obs Geoinf 26:156–175, Elsevier B.V. https://doi.org/10.1016/j.jag.2013.06.002

Singh RP, Srivastav SK (1990) Mapping of waterlogged and salt-affected soils using microwave radiometers. Int J Remote Sens 11(January 2015):1879–1887. https://doi.org/10.1080/01431169008955135

Taylor GR et al (1996) Radar imagery of saline soils using airborne. Remote Sens Environ 57(February 1995):127–142

Ug MVM, Ahmed Douaik TT (2008) Stochastic approaches for space–time modeling and interpolation of soil salinity. In: Metternicht G, Zinck JA (eds) Remote sensing of soil salinization: impact on land management. CRC Press, Boca Raton, pp 273–289

Wang Q, Li P, Chen X (2012) Modeling salinity effects on soil reflectance under various moisture conditions and its inverse application: a laboratory experiment. Geoderma 170:103–111, Elsevier B.V. https://doi.org/10.1016/j.geoderma.2011.10.015

Yu R et al (2010) Analysis of salinization dynamics by remote sensing in Hetao Irrigation District of North China. Agric Water Manag 97(12):1952–1960, Elsevier B.V. https://doi.org/10.1016/j.agwat.2010.03.009